Wind Tunnel Experiments on Cooling Tower Plumes: Part 1—In Uniform Crossflow

J. Andreopoulos[1]
Department of Mechanical Engineering,
The City College,
City University of New York,
New York, NY 10031

Measurements of velocity and temperature field and flow visualization results are reported for an ideal case of a cooling-tower plume in the presence of a uniform crossflow for various velocity ratios, densimetric Froude numbers, and Reynolds numbers. Coherent structures in the form of jetlike, wakelike, or mushroom-type vortices have been observed. The type of structure depends primarily on the velocity ratio. As the Reynolds number increases, turbulent structures appear, which have vorticity of the same sign as the partner vortices in the low Reynolds number case. The measurements showed that there is a strong interaction between the bending plume or jet and the wake of the cooling tower, which is basically responsible for the downwash effect. The latter is generally quite strong at low velocity ratios and high Reynolds numbers. High turbulence intensities are produced in the wake of the tower for a distance of 6 to 8 diameters. The plume is diluted faster as the velocity ratio increases and buoyancy decreases. In the wake region of the stack dilution increases with increased buoyancy.

1 Introduction

Cooling-tower systems of large power plants release their heat into the atmosphere either in the form of sensible heat or as a combination of latent and sensible heat. The amount of heat released over a small area can be very large. Thus, there is legitimate concern about the effect of such heat disposal on natural atmospheric processes and about its ecological impact. The most satisfactory method to assess the atmospheric effects of heat release is direct measurement. However, there are great difficulties in obtaining reliable field data. The major difficulty is that the atmospheric conditions change very quickly over the time the experiment is running, i.e., the initial and boundary conditions change rather irregularly. Therefore, it is now generally recognized that laboratory modeling of cooling-tower installations is an effective means of resolving questions related to plume behavior.

There is a great number of experimental studies on cooling-tower plumes in the literature, which reflects the importance in engineering application and atmospheric pollution. Such studies are described by Jain and Kennedy (1980), Mery et al. (1980), Violet (1977), and Slawson and Csanady (1971). In these studies an effort has been made fully or partly to simulate the phenomena as they occur in nature. These phenomena are rather complicated and include: (1) turbulence production, mixing, and transport, (2) buoyancy effects, (3) two phases, i.e., air and water, (4) the influence of the cross-stream atmospheric boundary layer. Policastro et al. (1980) compiled field measurements to evaluate the performance of mathematical models. Their study shows that the available measurements, which included visible plume outline, trajectory, and dilution, were not sufficient for a fair comparison with the existing models and calculation methods.

Few of the abovementioned studies, however, include reliable measurements of turbulence quantities throughout the flow. The aim, therefore, of the current experimental program is to increase the physical understanding of the flow. In addition, the present study has been motivated by the less than completely satisfactory predictive capability of current plume numerical or theoretical models. The absence of turbulence measurements, which are important to complete the picture, considerably hampers the development of calculation methods, since a realistic modeling of the turbulent stresses and heat or mass fluxes requires an understanding of the turbulence processes, especially in the present complex situation of plumes discharged into the atmosphere with the presence of a crossflow. Therefore, an additional aim to that of physical understanding of the flow is to obtain reliable turbulence data throughout the flowfield, which can be used for testing and improving calculation methods.

Along these lines a single-phase experiment has been considered here under neutral atmospheric conditions. A further simplification concerning the model has been made: The plume was issuing into the crossflow from a cylinder stack having a certain height H and diameter D (see Fig. 1), which is not the situation of a natural-draft cooling tower. In this paper, the experimental results are reported for the case of a uniform crossflow while in the accompanying paper by Andreopoulos (hereafter mentioned as paper 2) the results are reported for the nonuniform crossflow case.

In both cases the following effects have been studied:

(*i*) The effects of Reynolds number
(*ii*) The effects of velocity ratio
(*iii*) The effects of the densimetric Froude number.

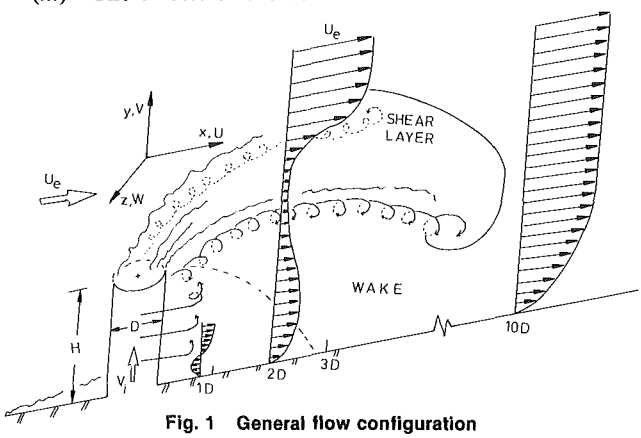

Fig. 1 General flow configuration

[1]Formerly at the Sonderforschungsbereich 80 of the University of Karlsruhe, Federal Republic of Germany.

Contributed by the Heat Transfer Division for publication in the JOURNAL OF HEAT TRANSFER. Manuscript received by the Heat Transfer Division March 11, 1988. Keywords: Flow Visualization, Plumes, Turbulence.

Each of the above parameters was varied while the other two remained constant. The study of the Reynolds number effects shows many important dynamic features in common with isothermal jets, while the study of the velocity ratio R indicated a considerable difference between low and high R plumes. The study of the densimetric Froude number effects was necessary to show how some important characteristics of the plume, like downwash, liftoff, spreading rate, etc., are affected by the stack densimetric Froude number.

The experimental program included a flow visualization study and mean and fluctuating velocity and temperature measurements with multiwire probes and thermocouples.

2 General Flow Configuration

The present flow is quite complicated in nature since it includes interaction of the jet flow, which is developing inside the pipe under circumferentially varying pressure gradient, with the free stream and the wake of the cylinder where the back pressure causes significant streamline curvature. A simplified picture of the jet as conceived from the present investigation, and previous work like that of Mousa et al. (1977), is shown in Fig. 1. The present flow is similar to the jet in the crossflow studies of Foss (1980), Keffer and Baines (1963), Crabb et al. (1981), Komotani and Greber (1972), Ramsey and Goldstein (1971), and Andreopoulos and Rodi (1984). The difference is that in these studies the jet was issuing from a circular outlet on a wall into a cross stream along the wall, while in the case of plumes the jet is issuing from a circular pipe that penetrates the cross stream by a height H.

The jet coming out of the pipe is bent by the cross stream while the latter is deflected by the jet in the normal and lateral direction. An important characteristic of the flow is that the shear layer emanating from the upstream edge of the cylinder is considerably thicker than that emanating from the downstream edge of the cylinder (lee side). The reason is that the former layer grows under the influence of an adverse pressure gradient while the latter is affected by a favorable pressure gradient. In fact, the annular boundary layer in the pipe has nonuniform thickness around the pipe circumference, which is a result of the continuously varying pressure gradient around the exit. Similar behavior has been found by Foss (1980) and Andreopoulos (1982) in the jet in a crossflow case, which can be considered as a limit of the present flow if $H = 0$. In these studies the exits of velocity profiles were found to be considerably distorted. Another similar feature between that flow and the present one is the existence of a pair of bound vortices with a "skew-induced" or pressure-driven secondary flow (Prandtl's first kind), which is due to the initially existing pipe flow vorticity, which is stretched and reoriented to give contributions in the longitudinal direction. The secondary motion induced by these vortices is responsible for the kidney shape of the bent-over jet and decays in the downstream direction under the action of the turbulent stresses.

There is, however, an important difference between the jet in a crossflow and the present one, namely that of the cylinder wake, which is responsible for the so-called "downwash" effect of the plume. This wake of the low aspect ratio cylinder and the bent-over jet interact strongly in a mutual way. There is also a wakelike region due to obstruction of the crossflow by the jet itself that is present in both cases and that seems to interact strongly with the wake of the solid body and to be more predominant than the wake of the cylinder.

There is also a reverse flow region in the wake, which is shown approximately in Fig. 1 as depicted from the flow visualization experiment and from tuft studies. In this region occasionally reverse flow can be expected, but it is not a closed recirculation zone where the instantaneous velocity vector always has a reverse direction. Therefore, it does not preclude certain careful use of the hot wire.

The ground level concentration of stack effluent downwind from a cooling tower is, for obvious reasons, of great importance. It depends on the strength of the downwash effect, which is the capture of stack effluent by the eddies on the lee side of the stack, and on the plume attachment or impingement on the ground. It turns out that the latter depends primarily on the velocity ratio and/or on the Reynolds number of the oncoming crossflow and secondarily on the jet densimetric Froude number. The downwash effect is a result of the flow separation behind the tower, which induces a sufficient under-pressure to bend the plume further downward. This drastically influences the location and the spreading of the plume even in the far field. Slawson et al. (1978) indicated that the far field trajectory can be shifted downward by up to 50 percent by downwash effects. In the near field this separation region causes increased mixing and increased entrainment of ambient fluid, which then entrains the plume. Generally, the flow picture in the wake of the tower is very complicated. Apart from the recirculation on the vertical plane, there is also a recirculation on the horizontal plane, which is caused by the shear layers separated from the external surface of the tower. These shear layers have the plume above them and they interact strongly with it. The present investigation shows that the wake of the plume is stronger than the wake of the tower and therefore, it is expected that some parts of the shear layers may be sucked into the wake of the plume and then entrain the plume.

At higher velocity ratios, neither downwash nor plume ground attachment is expected and the ground level concentrations of stack effluent should, therefore, be practically zero everywhere. At moderate velocity ratios, only downwash and no ground attachment is anticipated. At low velocity ratios, both downwash and plume attachment on the ground are expected.

3 Experimental Setup and Data Reduction

The measurements were made in the closed-circuit wind tunnel at the Sonderforschungsbereich 80, University of Karls-

Nomenclature

D = cooling tower inner diameter
Fr = densimetric Froude number = $V_j/(gD\,\Delta\rho/\rho_e)^{1/2}$
g = gravitational acceleration
H = cooling tower height above ground
R = velocity ratio = V_j/U_e
Re = Reynolds number = $U_e D/\nu$
$1/2\overline{q^2}$ = turbulent kinetic energy = $1/2\,(\overline{u^2} + \overline{v^2} + \overline{w^2})$
T = temperature
$\bar{U}, \bar{V}, \bar{W}$ = mean velocity components in x, y, z directions
u, v, w = velocity fluctuations about mean value
x, y, z = system of coordinates
β = volumetric expansion coefficient
Ω = vorticity vector

Subscripts

e = values at free stream of crossflow
j = values inside cooling tower

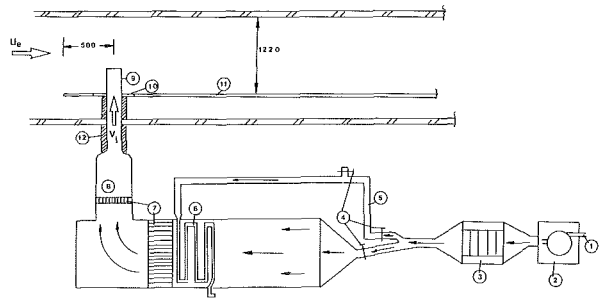

Fig. 2 Experimental arrangement: (1) flow valve; (2) two-stage compressor; (3) resistor box; (4) flow rate control valves; (5) bypass pipe; (6) heat exchanger; (7) flow straighteners; (8) settling chamber; (9) cylindrical cooling tower model; (10) turntable; (11) flat plate; (12) thermal insulation

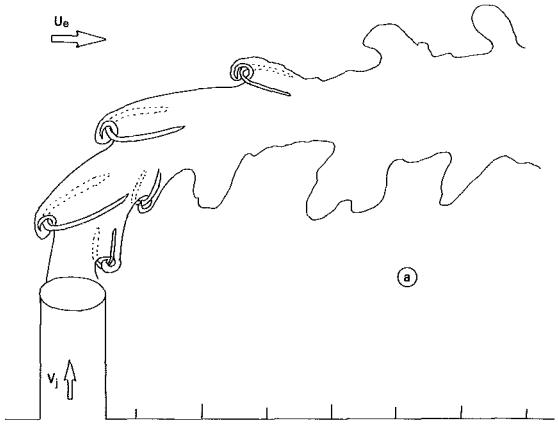

Fig. 3 Flow sketches for $R = 2.8$, Re = 2400, Fr = ∞

ruhe, which has an octagonally shaped working section 6 m long and 1.5 m in diameter, with an adjustable roof set to give zero pressure gradient. The experimental setup is illustrated in Fig. 2. A 6-m-long flat plate was installed 0.28 m above the tunnel floor. The size of the model was determined through a procedure described in Appendix A and selected to be 80 mm in internal diameter. This gave a geometric scale between the full size tower and the model of the order of 1:1000.

The jet/plume flow was supplied by the two-stage compressor 2 as shown in Fig. 2. The air flow leaving the compressor was heated in the box 3 by means of electrical resistors of total installed power of 19 kW. The resistors were controlled through automatic relays by the air flow valve 1 positioned at the compressor inlet. If the flow rate was extremely low, the resistors were automatically switched off to protect the installation from burning. To achieve high buoyancy forces, however, extremely high temperature and very low speeds were required. This was made possible by bypassing part of the flow to the heat exchanger 6 through the pipe 5. The valves 4 were used to control the flow rate in the model while the compressor was supplying air at the maximum rate. The whole heated-air supply was thermally insulated. A honeycomb 7 was used at two positions as flow straighteners. The last part of the model was made of brass pipe 2.5 mm thick and it was rotatable. Two models were used and their dimensions are shown in Table 1, together with the flow parameters. A total of five experiments have been carried out with different velocity ratios R, Reynolds numbers Re, and Froude numbers Fr. These experiments are intended to show the influence of the abovementioned parameters on the hydrodynamic field. Although the range of these parameters is rather limited, the results indicate that it is large enough to demonstrate significant changes in the flow structure.

Mean velocities and turbulence measurements were made with Constant Temperature Anemometers (CTA), DISA type 55M01, and home-made subminiature triple hot-wire probes with 5-μm wires. An effort has been made to keep the dimensions as small as possible. The probe consists of three single probes that have been constructed from ceramic tubes and stainless steel prongs.

Mean temperature and fluctuations were measured with a 1-μm "cold wire" mounted on probes clamped to the side of the triple-wire probe. The multiwire probe has a spatial resolution of 1.8 mm. The cold wire was operated by a Constant Current Anemometer (CCA), DISA type 55M01, with a temperature bridge. The heating current was not more than 0.15 mA and the temperature sensitivity was at least two orders of magnitude greater than the velocity sensitivity in all cases. The material of the wire was P1 + 10 percent Rd and its resistivity coefficient was measured to be between 0.00169 and 0.00170°C^{-1}. A typical value of the temperature sensitivity of a wire with $R = 70.52$ ohm at 20°C was 80 mV/°C. The noise level of the anemometer was of the order of 40 mV, which represents a temperature resolution no less than 0.5°C. Bearing in mind that the total initial temperature difference was roughly 110°C, this value of temperature resolution is very satisfactory. End-conduction effects were considered to be negligible because the length l over the diameter d of the wire was larger than 1000 (see Smits et al., 1978, and Lecordier et al., 1982). As a bonus the uncompensated frequency response of the anemometer increased to about 1.2 kHz and therefore, no further compensation was applied.

The four signals were digitized and stored on magnetic tapes for later data reductions. Thus, the instantaneous three velocity components *and* temperature were available simultaneously. The characteristic frequency of the large eddies was of the order of V_j/D, i.e., between 15 and 125 Hz, while the upper frequency limit is set by the spatial resolution of the probe, which was of the order of 1 to 2 kHz. Estimates of the viscous scales of the flow based on the dissipation rate of the turbulent kinetic energy, which was obtained by difference from the corresponding transport equation, indicated that the Kolmogorov length scale and passage time were of the order of 0.3 mm and 6 ms respectively. The Batchelor scale or temperature microscale is of the same order as the Kolmogorov length scale since the Prandtl number for air is close to 1.

All calibrations, which include velocity calibration, pitch and yaw calibration of the triple wire, and temperature calibration of the cold wire have been performed "in situ" and "on line" with the HP-1000 computer. It is, therefore, expected that gain problems are not present here.

The results include profiles of mean velocity and temperature, turbulent kinetic energy, shear stresses, and velocity-temperature correlations.

Finally, a flow visualization experiment has been carried out. The plume was visualized by introducing a fog of paraffin-oil droplets into the plenum chamber through a row of holes on a tube spanning the chamber width. The overpressure was small enough to ensure laminar flow. The photographic records were obtained with a cine-camera BOLEX model H-16 reflex with a rate of 46 frames per second. Negative prints have been also obtained from the cine-film and some of them are presented in Figs. 4 and 5.

Only a selection of the measured profiles and the flow visualization pictures will be presented here; further details are available in the departmental reports by Andreopoulos (1986a, 1986b).

4 Results

4.1 Instantaneous Structure. The flow visualization indicated the existence of coherent structures in the present flow for the first time. The type of structures depends primarily on the velocity ratio R.

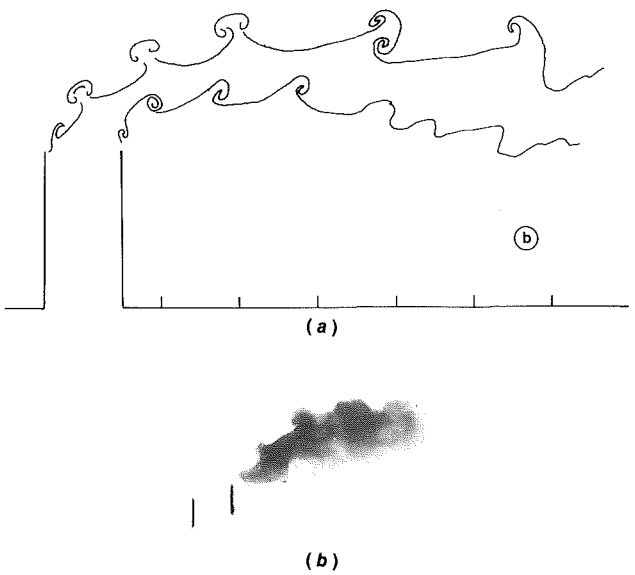

Fig. 4 (*a*) Flow sketch for the $R = 1$ case; (*b*) flow visualization of the $R = 1$, Re = 66,000, and Fr = ∞ experiment

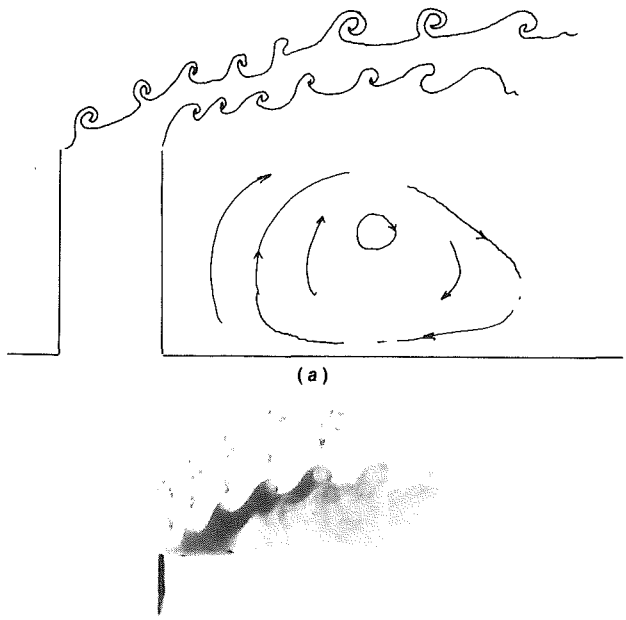

Fig. 5 (*a*) Flow sketch for the $R < 1$ case; (*b*) flow visualization of the $R = 0.2$, Re = 5800, and Fr = ∞ experiment

Figure 3 shows the observed flow structure for the case of $R \simeq 2.8$. The shear layers coming out of the pipe roll up at two different locations, i.e., at the upwind side and at the lee side of the pipe. If Ω_z is the vorticity of these rollings on the x-y plane, then Ω_z is positive in the vortices at the upwind side of the jet and negative in the vortices at the lee side of the jet. Although the vorticity of these rollings has the same sign as the vorticity of the layer inside the pipe, they do not belong to the same vortical ring, but they belong to two different vortices that are open at their legs, similar to those observed by Perry and Lim (1978) in their neutral buoyant jet and by Andreopoulos (1985) in the case of a jet in a crossflow. These vortices have jetlike structures and are a result of an instability phenomenon. The existing vorticity of the boundary layer inside the pipe plays a significant role in the formation of the vortices observed in these experiments. This vorticity is of the order V/δ where δ is the boundary layer thickness and V is a typical velocity just outside the boundary layer. Both V and δ were not uniformly distributed across the pipe exit. The boundary layer thickness δ was much smaller in the lee side of the pipe than in the upstream side while the opposite is true for the velocity V. Since the vorticity is proportional to δ^{-1} it may be expected that the existing vorticity in the pipe is greater in the lee side of the jet than in the upwind.

It is observed that the vortices at the upwind side of the jet are formed with the same frequency as the vortices on the lee side of the jet but with a considerable phase lag. The vortices on the lee side of the jet disappear very quickly while the others on the upwind side of the pipe persist much longer before they break down to turbulence. There are two reasons for this behavior: First, the streamlines in the wake region just behind the jet converge toward the plane of symmetry, resulting in a strongly negative gradient $\partial \bar{W}/\partial z$, which compresses the vortex lines and thus reduces the vorticity of the vortex; second, an important reason for weakening this vorticity is the strong turbulence in the wake of the cylinder and in the wake of the jet. Both effects contribute to the disappearance of the vortices on the lee side of the jet.

As the velocity ratio R is reduced, the flow structure changes significantly. Figures 4(*a*) and 4(*b*) show the instantaneous flow structure for $R = 1$. One striking feature of this flow is the appearance of mushroom-type vortices that are very regular. These vortices seem to be a result of superposition of vorticity shed from the inner surface of the pipe (i.e., originating from the shear layer inside the pipe) and vorticity of opposite sign, which exists in the crossflow shear layer separated from the outer surface of the pipe.

In this experiment wakelike vortices appear first on the upwind side of the pipe. These structures carry negative vorticity, i.e., opposite to that of the pipe flow. As they travel downstream another vortex is formed right behind them so that both appear to be on a mushroom-type vortical structure, which travels downstream.

At lower velocity ratios R, the flow pattern changed drastically. Figures 5(*a*) and 5(*b*) show a sketch and a flow visualization picture of the flow with $R = 0.2$. A row of wakelike vortices is formed in the upwind side of the pipe.

A row of jet-type vortices was also observed in the lower side of the jet. Pairing took place between two of them in the same row as well as between one of the lower row and one of the upper row of vortices.

As the Reynolds number increases (with R kept constant) the basic structure of the flow remain the same, but there is a considerable jitter among them.

Smoke was also observed to recirculate intermittently in the near-wake zone, for the small velocity ratio cases. The position of the center of this recirculation zone, which is not a closed recirculation zone, in the longitudinal direction depends strongly on the Reynolds number Re, while its position from the wall is a function of the velocity ratio. As the Reynolds number increases the center is formed closer to the pipe, while as the velocity ratio decreases it moves upward.

4.2 Time-Averaged Structure.

4.2.1 Mean Velocities. Figures 6(*a*) to 6(*c*) show the mean velocity vectors on the plane of symmetry $z/D = 0$ (where $W = 0$) for three of the five experiments shown in Table 1 at various downstream stations. The present flow is dominated by the mutual interaction of two low-pressure fields: the wake behind the bending-over jet and the wake of the cylinder. Their relative strength determines the general flow picture. There are two characteristic features that affect these two pressure fields and that ought to be mentioned: The higher the plume or the jet that penetrates the cross stream, the lower the pressure in the wake of the jet. This behavior has been verified in the jet-in-a-crossflow study of Andreopoulos (1982) where the wall static pressure has been measured for various velocity ratios.

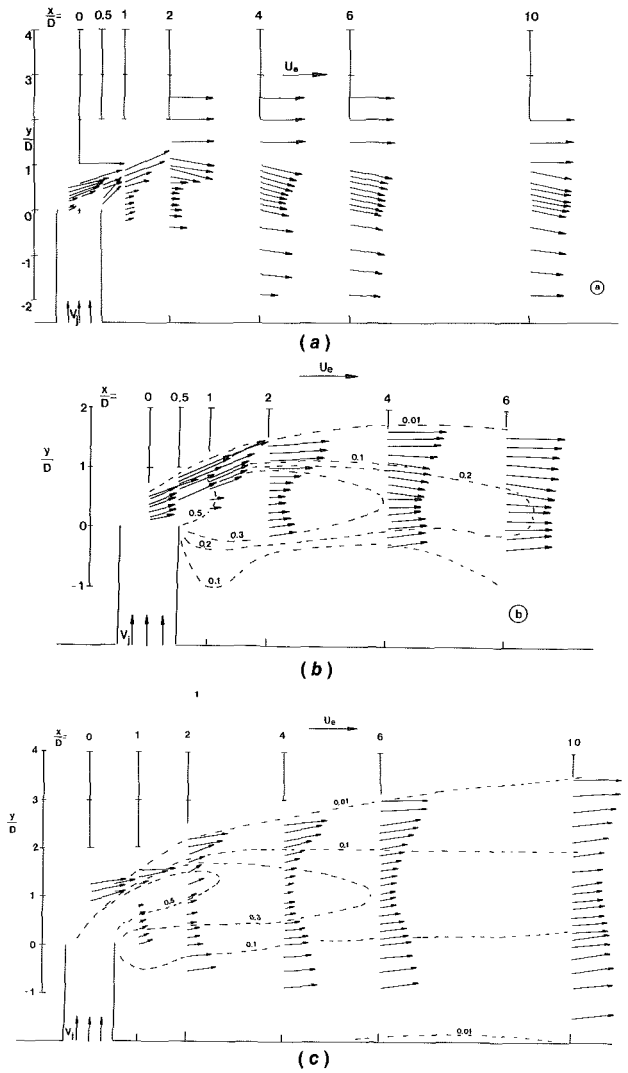

Fig. 6 (*a*) Mean velocity vectors on the plane of symmetry for the UFH1 experiment; (*b*) mean velocity vectors on the plane of symmetry for the UFH2 experiment; (*c*) mean velocity vectors on the plane of symmetry for the UFH4 experiment. Dotted lines: isotherms.

Similar arguments can be invoked for cylinders in a cross stream: the higher the aspect ratio of the cylinder, the stronger the low pressure in the wake.

Figure 6(*a*) gives the mean velocity vectors for the UHF1 experiment, which represents the highest Reynolds number case studied in the present investigation. The most important characteristic of this case is the downwash inclination of all velocity vectors downstream of the $x/D = 2$ location. This is not surprising since the bending over of the jet is considerably helped by the strong negative pressure in the near wake of the cylinder. It seems that, in this case, the wake of the cylinder dominates the flow behavior in the near field since it is stronger than the wake of the bending-over jet. As the Reynolds number decreases, the situation remains qualitatively the same but with large quantitative differences. This is shown in Fig. 6(*b*) where the mean velocity vectors are plotted for the UFH2 experiment, which has rather small buoyancy effects and the same velocity ratio as the UFH1 experiment but with considerably smaller Reynolds number. From Fig. 6(*b*) it is obvious that the vectors start to have a downwash inclination at $x/D = 4$ roughly, a distance larger than that of the flow of Fig. 6(*a*). This is in accordance with the general rule that indicates that length scales are reduced with increasing Reynolds number.

It seems that in the case of the UFH1 experiment the underpressure or rather the pressure coefficient in the wake of the cylinder is much lower than in the case of the UFH2 experiment for two reasons: first, because the aspect ratio of the cylinder is 25 percent higher in the UFH1 case than in the UFH2 experiment, and second, because the Reynolds number is higher. As a result of these two reasons, the bending over of the jet is faster in the UFH1 experiment than in the UFH2 experiment. In the latter experiment, the underpressure in the wake of the cylinder is weaker and seems that the low pressure in the wake of the bending over jet dominates the flow behavior. Apart from their low pressure, both wakes are characterized by strong acceleration of the flow in this region, which causes the fluid to rush to "fill" the wake. Thus, any nonzero inclination of the mean velocity vectors can be attributed to "filling" the wake effects and/or to low pressure effects. A few examples of these effects can be mentioned here: the upward motion at $x/D = 1$ in the wake of the cylinder in the UFH1 experiment (Fig. 6*a*) and at almost all downstream stations in the UFH2 experiment (Fig. 6*b*), is caused by the crossflow "filling" the wake of the bending over jet itself. The wake of the cylinder requires also "filling" by the cross flow. This is evident in the downstream profiles of Fig. 6(*a*) where the velocity vectors below the height of the exit plane increase with downstream distance.

Figure 6(*c*) shows the mean velocity vectors of the UFH4 experiment, which has a considerable amount of buoyancy forces. The Reynolds number and the velocity ratio R are roughly the same as those of the UFH2 experiment. Consequently, Fig. 6(*c*) should be directly compared to Fig. 6(*b*). There are two striking features in Fig. 6(*c*): One is the deeper penetration of the buoyant jet in the cross stream, which results in smaller velocities than the partner nonbuoyant flow (UFH2 experiment) because the jet is spread into larger regions in the y direction. The second feature is that almost all the velocity vectors are inclined upward even in regions close to the ground, where everything has been lifted off due to the low pressure in the wake of the jet and to the flow "filling" the wake of the jet as the conservation of the mass flow requires.

It seems that the wake of the jet is much stronger than the wake of the cylinder because the plume penetrates into the crossflow deeper, and therefore dominates the flow. Another reason for the upwash inclination of the velocity vectors is the secondary flow induced by the "bound" vortex is stronger when the plume penetrates the cross flow deeper.

The present measurements and the flow visualization did not show any recirculating fluid in the wake of the jet having a counterclockwise rotation. However, such a recirculation has been found in the experiments of Violet (1979) as well as in the calculations of Demuren and Rodi (1984) for $R = 1.7$ only. This ties up with the previously mentioned observation of the present study that the wake effects of the plume or jet become much stronger when the jet or plume penetrates the cross stream deeper, as is the case with high velocity ratio or strong buoyancy. At lower velocity ratios the calculations show characteristics similar to those observed in the present experimental investigation.

4.2.2 Mean Temperatures. Mean temperature is probably one of the most reliable quantities to measure even in regions of high turbulence intensities, such as the wake region behind the cylinder, because temperature is a scalar quantity and because temperature probes are more or less insensitive to flow direction. The latter may be important for an intrusive method of measuring temperature since such a probe can affect the flow field, which in turn alters the thermal field. To ensure that such effects are negligible, the probe has been yawed and pitched quite a few times without any significant change in mean temperature.

Figures 7(*a*) and 7(*b*) show some contours of isotherms plotted from the mean temperature measurements of the UFH2,

UFH3, UFH4, and UFH5 experiments. The isotherms correspond to values of the measured excess temperature $T - T_e$ normalized by the initial temperature difference $T_j - T_e$. Figure 7(*a*) shows the results of the UFH2 and UFH4 experiments with $R = 0.5$ and Fig. 7(*b*) contains the isotherms of the UFH3 and UFH5 experiments with $R = 0.2$. These results indicate that the plume is diluted faster as the velocity ratio increases and the Froude number increases (buoyancy decreases). In the wake region, however, dilution is high with higher buoyancy.

There is also evidence from these figures that the downwash effect is larger in Fig. 7(*b*). This indicates that this effect is stronger at low velocity ratios and high Froude numbers. In Fig. 7(*b*) Violet's (1977) results are plotted for comparison with the present results of the same velocity ratio R. His results, however, have been obtained at Fr = 0.8. Therefore, it is expected that his plume should have penetrated more into the cross stream than the present plume, with Fr = 3.3. However, this is not the case. There are several reasons for this disagreement. The first reason is that their boundary layer developed by the cross stream over the flat plate was very thick, of the order of $1H$. This could cause a faster spreading of the lower part of the plume. The second reason is that his model had an aspect ratio $H/D = 1.64$, which is smaller than the present one of 2, a fact that causes weaker low pressure in the wake of the cylinder. The third reason is the difference in Reynolds number. Their Reynolds number was 40,000 while the present one was only 15,500. In fact, the present experiment UFH1 showed that the higher the Reynolds number the stronger the downwash effect, i.e., the bending over of the jet takes place more quickly as the Reynolds number increases. The last reason is the internal inconsistencies of their data. Their concentrations obtained at low Reynolds numbers and at large streamwise distances are about 10 percent lower than those measured at high Reynolds numbers. It appears, therefore, that the disagreement between the present results and those of Violet (1977) is due to a combination of the above effects.

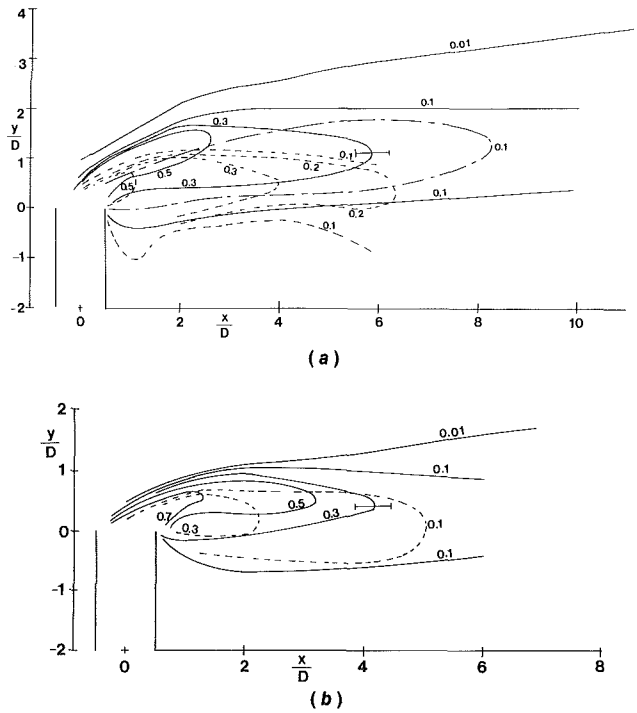

Fig. 7 (*a*) Contours of isotherms at $z/D = 0$: ——, UFH2 experiment; -----, UFH4 experiment; —·—, Violet (1977) experiment; (*b*) contours of isotherms at $z/D = 0$: ——, UFH3 experiment; ·····, UFH5 experiment

The present results indicate that dilution of the plume is strongly affected by the velocity ratio R and buoyancy. Dilution is defined as the inverse of the normalized excess temperature. The downstream extent of the isotherms and the area they confine indicate the ability of the plume to dilute its initial concentration of smoke or other species. A comparison between the UFH2 and UFH4 data indicates that dilution decreases with increased buoyancy. The same conclusion can be reached by looking at the isotherms. They clearly indicate that increased buoyancy reduces the dilution of the plume, except in the region of the wake of the cylinder, where the data show that the plume dilution is increased by buoyancy. This result is in contrast to the observed behavior in vertical buoyant jets (see Chen and Rodi, 1980). It can be attributed to the interaction of the bent-over plume or jet with its wake and the wake of the cylindrical stack. Both wakes are regions of high turbulence intensities that affect the heat transfer in the lower extent of the plume or jet by changing the lateral/normal diffusion and the entrainment rate. This interaction is strong when the penetration of the jet or plume into the cross stream is small. Therefore it is not surprising that dilution increases with decreasing buoyancy for small velocity ratios. As the velocity ratio increases the flow penetrates more into the cross stream and the jet-wake interaction is weaker than in the cases of small R. Thus a change in the abovementioned dependency of the dilution on buoyancy may be expected.

4.2.3 Turbulent Kinetic Energy. The most characteristic turbulent quantity is the turbulent kinetic energy $1/2\,\overline{q^2}$, which is plotted in Figs. 8(*a*) to 8(*c*) for three of the experimental cases shown in Table 1.

The experimental results of the UFH1 experiment are shown in Fig. 8(*a*). The first two profiles look like the distribution of $\overline{q^2}$ in a pure shear layer. However, the distribution of $\overline{q^2}$ is governed by an interaction of different mechanisms of production through various mean velocity gradients, notably $\partial\bar{U}/\partial y$, $\partial\bar{V}/\partial x$, $\partial\bar{W}/\partial z$, $\partial\bar{U}/\partial z$, and by mean and turbulent transport from the upstream pipe flow. It appears, however, that in the region above the exit the production due to the mean velocity gradient $\partial\bar{U}/\partial y$ is the dominant process because $\overline{q^2}$ has a maximum around the position of maximum $\partial\bar{U}/\partial y$.

At the downstream stations $x/D = 1$ and 2 a second peak in $\overline{q^2}$ starts to develop inside the wake of the cylinder, which grows up very quickly at further downstream positions. Between the two peaks, there is a region of lower turbulence kinetic energy, which corresponds to the minimum of the mean velocity distribution in the wake of the plume. However, this region seems to disappear at the next station $x/D = 4$, where

Table 1 Flow parameters for the hot-wire measurements

Experiment	H, mm	D, mm	$\frac{H}{D}$	U_e, m/s	V_j, m/s	$R = \frac{V_j}{U_e}$	$\mathrm{Re} = \frac{U_e D}{\nu} \times 10^5$	T_e, °C	T_j, °C	$\mathrm{Fr} = \frac{V_j}{\sqrt{gD\,\Delta T/T_j}}$
UFH1	200	80	2.5	21	10.5	0.5	1.11	20	20	∞
UFH2	160	80	2.0	2.58	1.29	0.5	0.135	20	28.55	8.681
UFH3	160	80	2.0	6.48	1.29	0.2	0.339	20.2	29.1	8.624
UFH4	160	80	2.0	2.96	1.48	0.5	0.15	19.7	121.0	3.295
UFH5	160	80	2.0	7.50	1.5	0.2	0.332	20.0	132.0	3.22

the outer peak is hardly distinguishable, while at $x/D = 6$ it has completely disappeared. Since the turbulent kinetic energy produced in the wake seems to be twice as much as that produced in the shear layer a great part of the wake turbulence is expected to diffuse outward in the normal direction.

At $x/D = 1$ one more peak is evident at about $y/D \simeq 0$, followed by a change of sign in $\overline{uv}$ (not shown here). This may be attributed to the shear layer emanating at the downstream edge of the cylinder where the shear stress is positive. The turbulent kinetic energy reaches a maximum at $x/D = 4$ in the wake region and then it starts to decay continuously. Profiles of $\overline{q^2}$ at $z/D = -0.5$ are also shown in Fig. 8(*a*). At $x/D = 2$, two peaks are distinct. The first one, in the shear layer region, is associated with the velocity gradient $\partial\bar{U}/\partial y$, while the second takes place in a region where $\partial\bar{U}/\partial y$ is very small. In general, the $\overline{q^2}$ profiles off the plane of symmetry at $x/D = 2$ are much larger than those at the plane of symmetry $z/D = 0$. In fact the second maximum in the wake region is about 70 percent larger than that at $z/D = 0$. These high values of q^2 in the region of the cylinder wake are due to the high velocity gradient $\partial\bar{U}/\partial z$ and the $\overline{uw}$ correlation. The term $\overline{uw}\,\partial\bar{U}/\partial z$ is zero on the plane of symmetry and out of this plane can reach values up to $10^{-2}\,U_e^3/D$. It seems, therefore, plausible that this large production is transported by diffusion toward the plane of symmetry and then upward toward the wake of the jet or directly upward.

Similar features indicate the profiles of $\overline{q^2}$ of the UFH2 experiment shown in Fig. 8(*b*), although measurements inside the wake region of the cylinder have not been extended. The peak on the shear layer side is slightly larger in magnitude than that of the UFH1 experiment, which may be attributed to Reynolds number effects. A minimum can be also observed in the region of the wake of the plume, which does not persist more than $2D$ downstream. It seems that this minimum is a result of small production by $\partial\bar{U}/\partial y$ and increased destruction by $\partial\bar{U}/\partial z$, which is positive but with $\overline{u^2} > \overline{v^2}$. At the same time, the streamline convergence on the zox plane associated with the $\partial\bar{W}/\partial z$ gradient suppresses turbulent production too.

Farther downstream $\partial\bar{W}/\partial z$ becomes weaker while $\partial\bar{U}/\partial x$ is still significant. It therefore seems plausible that the main reason for the disappearance of this low $\overline{q^2}$ region is an excessive diffusion of turbulent kinetic energy coming out from the wake of the cylinder.

For the UFH4 experiment with significant buoyancy the $\overline{q^2}$ profiles are shown in Fig. 8(*c*). As in the case of the mean velocities, the $\overline{q^2}$ profiles do not vary much with longitudinal distance. The double peak behavior of the $\overline{q^2}$ profiles, which seems to persist more than $6D$ in the downstream direction, is associated with the $\partial\bar{U}/\partial y$ and $\partial\bar{U}/\partial z$ gradients. The peak in the wake of the cylinder is slightly larger than the same peak in the UFH1 experiment behavior, which is due to Reynolds number effects.

The effects of buoyancy on $\overline{q^2}$ can be characterized as direct and indirect. A direct effect on the turbulent kinetic energy production is the extra term of production due to buoyancy, namely $\beta g\overline{v\vartheta}$, which represents an exchange between $\overline{q^2}$ and potential energy. The increase of length scale and spreading indirectly affect turbulence production, since they alter first the velocity gradients, which in turn affect the production of $\overline{q^2}$ by shear. This seems to be the reason why the peak on the outer shear layer in the UFH4 experiment is considerably smaller than the peak in the UFH2 experiment. Buoyancy decreases the $\partial\bar{U}/\partial y$ gradient, which turns out to be the major contributor to the turbulent kinetic energy production despite the fact that the situation in this part of the plume in terms of stratification is unstable, and therefore, direct effects of buoyancy should be important because $\partial\bar{T}/\partial y < 0$.

A detailed discussion of the behavior of all the terms appearing in the transport equation of turbulent kinetic energy

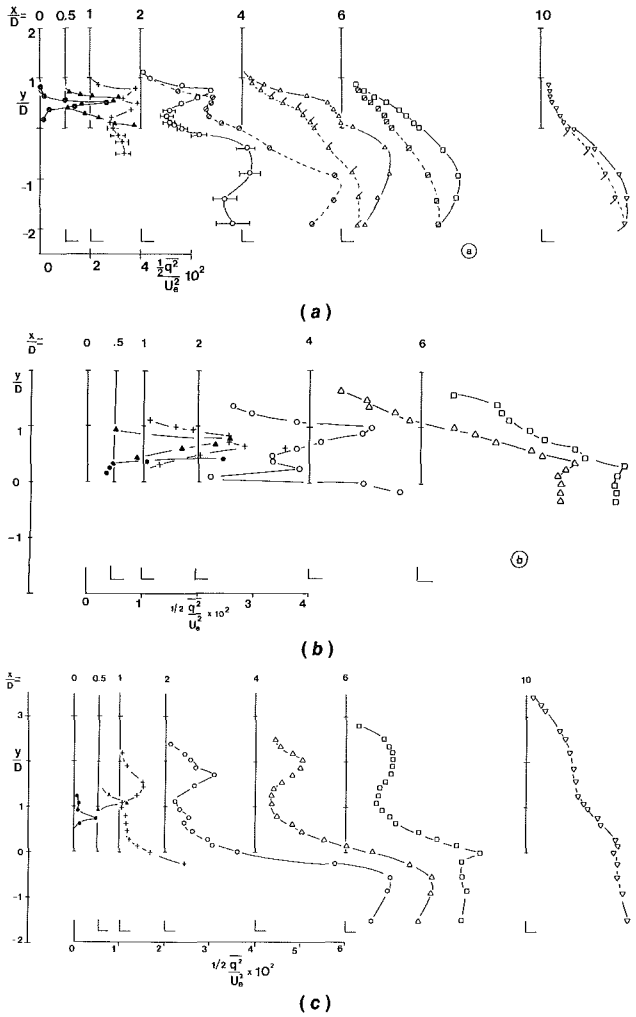

Fig. 8 (*a*) **Turbulent kinetic energy profiles for the UFH1 experiment; symbols: •, $x/D = 0$; ▲, $x/D = 0.5$; +, $x/D = 1$; ○, $x/D = 2$; △, $x/D = 4$; □, $x/D = 6$; ▽, $x/D = 10$; solid line through symbols: $z/D = 0$; dotted line through symbols: $z/D = 0.5$ (flagged symbols);** (*b*) **turbulent kinetic energy profiles for the UFH2 experiment (symbols as in Fig. 8*a*);** (*c*) **turbulent kinetic energy profiles for the UFH4 experiment (symbols as in Fig. 8*a*)**

that have been estimated from the present measurements is given in the reports by Andreopoulos (1986a, 1986b).

5 Conclusions

The present detailed measurements and flow visualization studies on the behavior of jets or plumes issuing into a cold cross stream through a cylindrical protrusion establish and document the flow dependence on the velocity ratio R, the Froude number Fr, and the Reynolds number Re. Coherent structures in the form of vortices have been observed in the present flow without any externally imposed excitation and classified, for the first time, according to the velocity ratio. In flows with $R > 1$ jetlike vortices appear in the upstream side of the cylindrical stack and remain well organized for the distance of a few diameters before breakdown to turbulence. For $R < 1$ wakelike vortices are formed, and for $R \simeq 1$ heterostrophic vortices in the form of a mushroom are present. While this describes the structure of the flow in the outer edge of the bending-over jet, jetlike vortices are formed in the lower edge of the jet, which break down to turbulence very soon due to the turbulence in the wake of the stack or the jet and to the vortex-line compression.

As the Reynolds number increases beyond the value of 6000, turbulent structures appear, which carry vorticity of the same sign as the partner vortices in the low Reynolds number case

of the same velocity ratio. The vorticity in these structures and/or vortices is attributed to a reorientation stretching or diffusion of the original pipe flow vorticity and also to vorticity of the shear layer separated from the outer surface of the cylindrical stack. Finally, pairing seems to be the mechanism for growing of the vortical structures or vortices.

The measurements showed that there is a strong interaction between the bending-over jet, its wake, and the wake of the cylinder. The low pressure in these wakes induces a lateral inward motion and also a downwash of the bent-over plume or jet. The latter, known as the downwash effect, is quite strong at low velocity ratios and high Reynolds numbers.

For all velocity ratios a shear layer with significant gradients of the streamwise velocity forms above the wake. As one proceeds downstream, the wake is "filled up" by the inward motion and the velocity gradients in the shear-layer and wake regions become smaller. High turbulent kinetic energy is produced in the wake of the cylinder, which is diffused toward the plane of symmetry and upward. This is due to high values of the lateral gradient of the longitudinal mean velocity component. Buoyancy production has a stabilizing effect in the wake region of the cylinder and it has a destabilizing effect, i.e., enhances turbulence production, at $y/D > 0$. The indirect effects of buoyancy are also large: The mean temperature and velocity profiles are dramatically changed by buoyancy. The spreading rate increases with buoyancy and the plume is diluted faster as the velocity ratio and buoyancy decrease. In the tower wake, increased buoyancy increases plume dilution.

Acknowledgments

The financial support of the Deutsche Forschungsgemeinschaft is gratefully acknowledged.

References

Andreopoulos, J., 1986a, "Wind Tunnel Experiments on Cooling Tower Plumes. Part I," Report No. SFB 210/E/18, University of Karlsruhe, Federal Republic of Germany.

Andreopoulos, J., 1986b, "Wind Tunnel Experiments on Cooling Tower Plumes. Part II," Report No. SFB/E/19, University of Karlsruhe, Federal Republic of Germany.

Andreopoulos, J., 1985, "On the Structure of Jets in a Cross-Flow," *J. Fluid Mech.*, Vol. 157, pp. 167–197.

Andreopoulos, J., 1982, "Measurements in a Jet-Pipe Flow Issuing Perpendicularly Into a Cross Stream," ASME *J. Fluid Engrg.*, Vol. 104, pp. 493–499.

Andreopoulos, J., and Rodi, W., 1984, "Experimental Investigation of Jets in a Crossflow," *J. Fluid Mech.*, Vol. 138, pp. 93–127.

Chen, C. J., and Rodi, W., 1980, *Vertical Turbulent Buoyant Jets*, Pergamon Press, New York.

Crabb, D., Durao, D. F. G., and Whitelaw, J. H., 1981, "A Round Jet Normal to a Cross Flow," ASME *J. Fluids Engrg.*, Vol. 103, pp. 142–152.

Demuren, A. O., and Rodi, W., 1984, "Three Dimensional Numerical Calculations of Flow and Plume Spreading Past Cooling Towers," 4th IAHR Cooling Tower Workshop, Interlaken, Oct. 1–5.

Jain, S., and Kennedy, J. F., 1980, "Physical Modeling of Cooling Tower Plumes," I.A.H.R. Cooling Tower Workshop, Sept. 21–25.

Foss, J., 1980, "Interaction Region Phenomena for the Jet in a Cross-Flow Problem," Rept. SFB 80/E/161, University of Karlsruhe, Federal Republic of Germany.

Keffer, J. F., and Baines, W. D., 1963, "The Round Turbulent Jet in a Cross Wind," *J. Fluid Mech.*, Vol. 15, pp. 481–496.

Komotani, Y., and Greber, I., 1972, "Experiments of Turbulent Jet in a Cross Flow," *AIAA J.*, Vol. 10, pp. 1425–1429.

Lecordier, J. C., Paranthoen, P., and Petit, C., 1982, "The Effect of the Thermal Prong-Wire Interaction on the Response of a Cold Wire in Gaseous Flows," *J. Fluid Mech.*, Vol. 124, pp. 457–473.

Maskell, E. C., 1965, "A Theory on the Blockage Effects of Bluff Bodies and Stalled Wings in a Closed Wind Tunnel," ARC R@M 3400.

Mery, P., Caneill, J. Y., Hodin, A., and Saab, A., 1980, "Dry Cooling Towers, Thermodynamic and Microphysical Impact of a 1000 MW Source Released in the Atmosphere," I.A.H.R. Cooling Tower Workshop, Sept. 21–25.

Morrison, G. L., 1974, "Effects of Fluid Property Variations on the Response of Hot-Wire Anemometers," *J. Physics E: Sci. Instrum.*, Vol. 7, pp. 434–436.

Moussa, Z. M., Trischka, J. W., and Eskinazi, S., 1977, "The Near Field in the Mixing of a Round Jet With a Cross Stream," *J. Fluid Mech.*, Vol. 80, pp. 49–80.

Perry, A. E., and Lim, T. T., 1978, "Coherent Structures in Coflowing Jets and Wakes," *J. Fluid Mech.*, Vol. 88, pp. 451–463.

Perry, A. E., Lim, T. T., and Chong, M. S., 1979, "Critical Point Theory and Its Application to Coherent Structures and the Vortex Shedding Process," Rept. FM-11, University of Melbourne, Australia.

Policastro, A. J., Carhart, R. A., Ziemer, S. E., and Haake, K., 1980, "Evaluation of Mathematical Models for Characterizing Plume Behavior From Cooling Towers," NUREG/CR-1581, Vol. 1, RB, R6.

Rae, W. H., and Pope, A., 1984, *Low Speed Wind Tunnel Testing*, Wiley, New York.

Ramsey, J. W., and Goldstein, R. J., 1971, "Interaction of a Heated Jet With a Deflecting Stream," ASME JOURNAL OF HEAT TRANSFER, Vol. 93, pp. 365–372.

Slawson, P. R., Coleman, J. H., and Frey, J. W., 1978, "Natural Draft Cooling Tower Plume Behavior at Paradise Steam Plant," Tennessee Valley Authority, Chattanooga, TN.

Slawson, P. R., and Csanady, G. T., 1971, "The Effect of Atmospheric Conditions on Plume Rise," *J. Fluid Mech.*, Vol. 47, pp. 33–49.

Smits, A. J., Perry, A. E., and Hoffman, P. H., 1978, "The Response to Temperature Fluctuations of a Constant-Current Hot-Wire Anemometer," *J. Physics E: Sci. Instrum.*, Vol. 11, pp. 909–914.

Viollet, L., 1977, "Etude de Jets dans des Courants Traversiers et dans des Millieux Stratifies," Report Electricite de France, Chatou, France.

Vrettos, N., 1984, "Experimentelle Untersuchung der Ausbreitung von Kuhlturmschwaden in Windkamal," Diplomarbeit, Institut fur Hydromechanik, University of Karlsruhe, Federal Republic of Germany.

APPENDIX

The size of the model was determined by considering the following requirements for the flow: First, a Reynolds number of the order of 10^4 should be achieved; second, a low densimetric Froude number flow should also be accomplished; third, the velocity ratio should be in the range $0.2 \leq R \leq 0.5$; fourth, distortion of the near and far field of the flow due to blockage should be minimal. In addition to these requirements a restriction on the maximum temperature difference had to be applied for safety reasons: $\Delta T = T_j - T_e = 110°C$ and therefore $\Delta T/T_j = 0.848$ for $T_e = 20°C$. The variation of Fr^2 with the pipe diameter D is shown in Fig. A1 for various values of U_e. On each of these lines the minimum value of D that corresponds to $Re = 10^4$ is marked. Blockage effects were calculated according to Maskell's theory (1965) given by Rae and Pope (1984): $\Delta V/V = 0.25\, A_m/A_w$ where ΔV is the velocity increment due to blockage, V is the velocity, A_m is the model frontal area, and A_w is the wind tunnel cross-sectional area. Since investigation of the far-field development was also part of this program, it was decided that velocity increment beyond the range of 0.2 percent of the free-stream velocity, which in fact is the level of free-stream turbulence in the tunnel, was not acceptable. For $H = 2D$, $A_m = 2D^2$ and $A_w = 1.44\ m^2$. Figure A1 indicates a typical variation of the parameters involved in the design of the present facility.

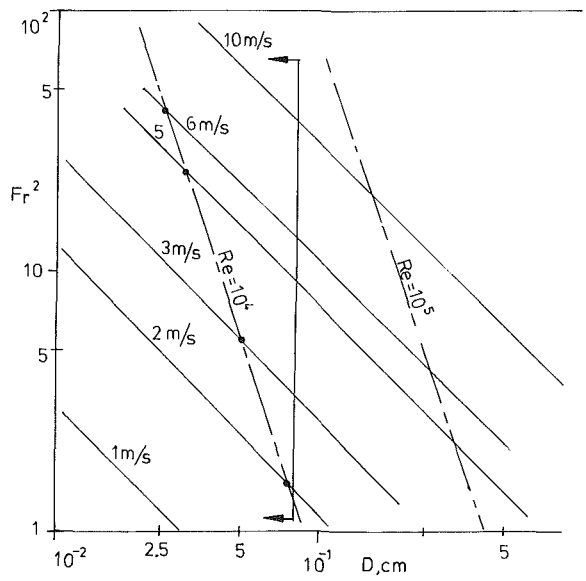

Fig. A1 Typical variation of Fr^2 versus D for $R = 0.5$ and $DT/T_j = 0.848$